J. Fluid Mech. (1971), *vol.* 46, *part* 2, *pp.* 321–335
Printed in Great Britain

Influence of surface roughness on the cross-flow around a circular cylinder

By ELMAR ACHENBACH
Institut für Reaktorbauelemente der Kernforschungsanlage, Jülich GmbH

(Received 1 June 1970)

The influence of surface roughness on the cross-flow around a circular cylinder is the subject of the present experimental work. The investigations were carried out in a high-pressure wind tunnel, thus high Reynolds numbers up to $Re = 3 \times 10^6$ could be obtained. Local pressure and skin friction distributions were measured. These quantities were evaluated to determine the total drag coefficient and the percentage of friction as functions of Reynolds number and roughness parameter. In addition the local skin friction distribution yields the angular position of boundary-layer transition from laminar to turbulent flow and the location of boundary-layer separation.

1. Introduction

Heat transfer and pressure drop of heat exchangers working in nuclear reactors are generally influenced by the surface roughness of the tubes because of the high Reynolds numbers, which are necessary for eliminating heat from the core. The present results referring to the cross-flow around a rough circular cylinder are preliminary investigations to classify roughness in an appropriate system. The experiments are carried out in a range of Reynolds numbers $4 \times 10^4 < Re \leqslant 3 \times 10^6$. Thus a comparison with the results of Fage & Warsap (1930) is possible; they tested the influence of roughness from $Re = 2{\cdot}5 \times 10^4$ to $Re = 2{\cdot}5 \times 10^5$. On the other hand new results are available for the transcritical flow régime, as the actual investigations exceed the range studied by Fage & Warsap by the factor 10.

Local pressure and skin friction distributions were measured. In rough square ducts the probes were calibrated and then transplanted to the test cylinders. This was possible by using emery papers as rough surfaces. In that way two roughnesses were tested. In a later run a third additional roughness realized by gluing 2·5 mm spheres on the surface was investigated. Unfortunately for this case there was no facility to calibrate the skin friction probe installed, so skin friction distribution can only be evaluated qualitatively.

The integration of the local values of static pressure and skin friction yields the total drag coefficient c_d. Furthermore one gets knowledge of boundary-layer separation and transition from laminar to turbulent flow.

2. Experimental arrangement

The experimental apparatus has already been described by Achenbach (1968) in a previous paper, which deals with investigations on the cross-flow past a smooth circular cylinder. To facilitate short information the most important details are repeated in the form of a table:

Wind tunnel	Closed atmospheric circuit, alternatively high pressure wind tunnel
Test section	Cross-section: 500×900 mm
Test cylinder	Diameter $D = 150$ mm, length $l = 500$ mm
Fluid	Air of $T = 60\,^{\circ}\mathrm{C}$ at static pressure of $1 \leqslant p_{\mathrm{stat}} \leqslant 40$ bar
Turbulence level	$Tu \approx 0{\cdot}7\,\%$ in the free air stream

3. Measurement techniques and calibration procedure

In principle the determination of local static pressure and skin friction can be verified in the same way as it was done for the cylinder with a smooth surface. Both probes are mounted at the same generator line of the test cylinder, which could be rotated around its longitudinal axis. However, the manufacturing of the rough surface by gluing emery paper leads to some difficulties in installing and calibrating the skin friction probe.

The principle of this probe, which is shown in figure 1, is based on the measurement of the pressure difference at an edge, which transversely projects only some hundredths of a millimetre into the boundary layer. If the height h of the probe is low enough, the quantity of the pressure difference Δp_e depends on the wall shear stresses τ_0 only. With respect to the very small size of the edge it must be taken into account that the surroundings of the probe must not be changed during the time from calibration to measurement. As we saw no possibility to carry out the calibration at the rough surface of the test cylinder, we had to transplant the probe with its surroundings into a known flow. The way of doing this is described below.

The skin friction probe and the tap for the static pressure are fixed at a thin steel foil (0·15 mm). The length of this foil is equal to the circumference πD and the width is equal to the diameter D of the test cylinder (figure 2(*a*)). This test foil is covered with a selected emery paper, which represents the roughness to be investigated.

In a second step (figure 2(*b*)) the test foil is mounted into a square duct, which is covered inwards with the same emery paper. The rough-channel flow was taken as the calibration standard of the probe. The advantage of an easy transplantation from channel to cylinder, compared with the circular tube, is paid with the difficulties resulting from the secondary flow in the square duct; for here the distribution of wall shear stresses is not uniform at the circumference of the channel cross-section. Therefore the skin friction profile must be determined. For this purpose a Preston tube was calibrated in a corresponding rough

circular tube before applying it to the channel flow. Figure 3 shows an example of the results of skin friction distribution in the square duct discussed later on. With these values of local skin friction available the probe could be calibrated.

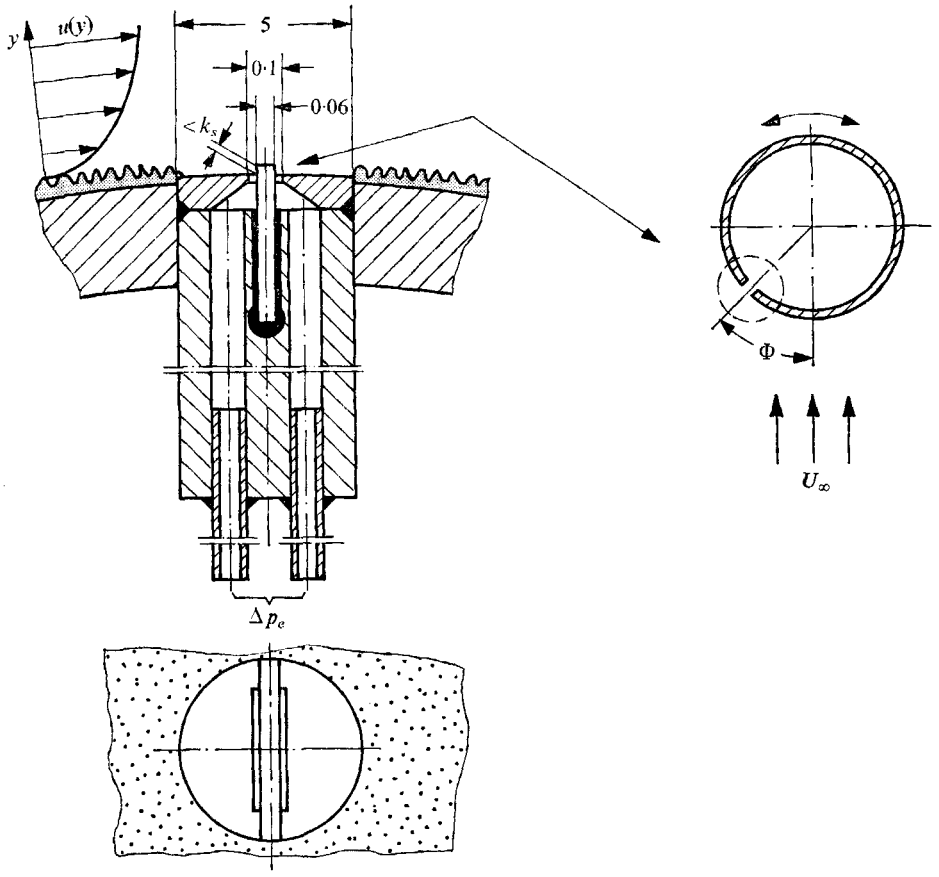

FIGURE 1. Skin friction probe, detail. Dimensions in millimetres.

The dimensionless presentation of the calibration curve has the form

$$\Delta p_e/\tau_0 = f(\Delta p_e h^2 \rho/\eta^2;\ k_s/h), \tag{1}$$

where h is the height of the edge, k_s Nikuradse's sand-grain roughness, ρ the fluid density and η the fluid viscosity. As the geometrical parameters h and k_s must not be changed within each arrangement, their influence can be described by a constant, which is implicitly contained in the calibration curve. For this case (1) simplifies in the following way:

$$\Delta p_e/\tau_0 = f(c(\Delta p_e \rho/\eta^2)). \tag{2}$$

The constant c has the dimension m^2.

On the other hand the channel test yields the friction factor of the square duct

$$\psi = \frac{\Delta p}{\frac{1}{2}\rho \bar{U}^2 (L/D)} \tag{3}$$

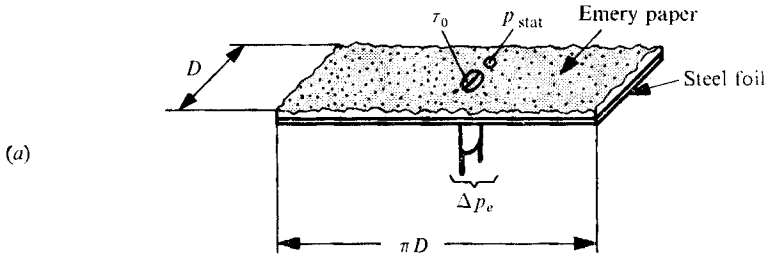

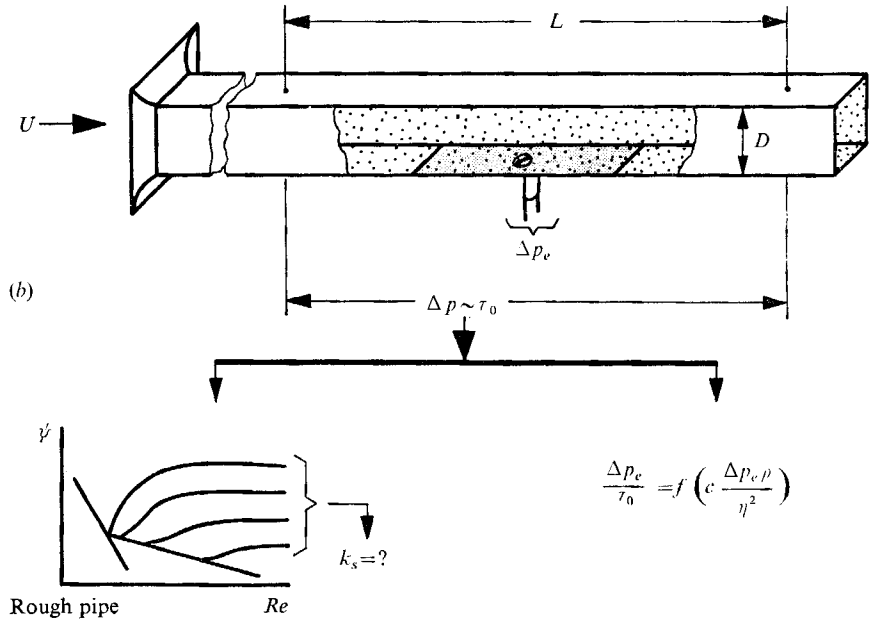

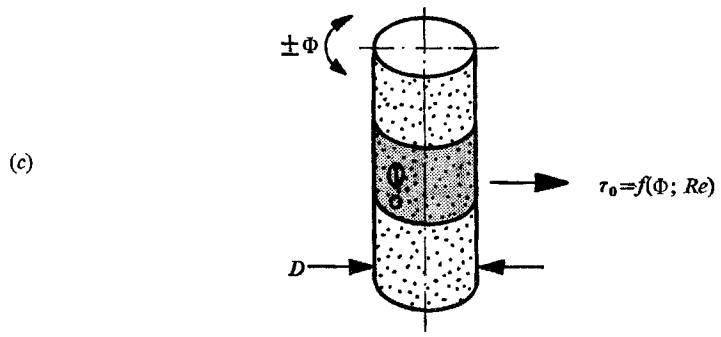

FIGURE 2. Calibration procedure of the skin-friction probe.

as a function of Reynolds number, where L is the length and D the hydraulic diameter of the duct. Plotting this result into Nikuradse's diagram for the flow through rough pipes (Nikuradse 1933) the equivalent sand-grain roughness of the present roughness combination can be determined (figure 5).

In a last step the test foil, prepared with the calibrated skin friction probe, is transplanted to the test cylinder (figure 2(*c*)).

Of course, the calibrating procedure just described must be repeated for each roughness investigated.

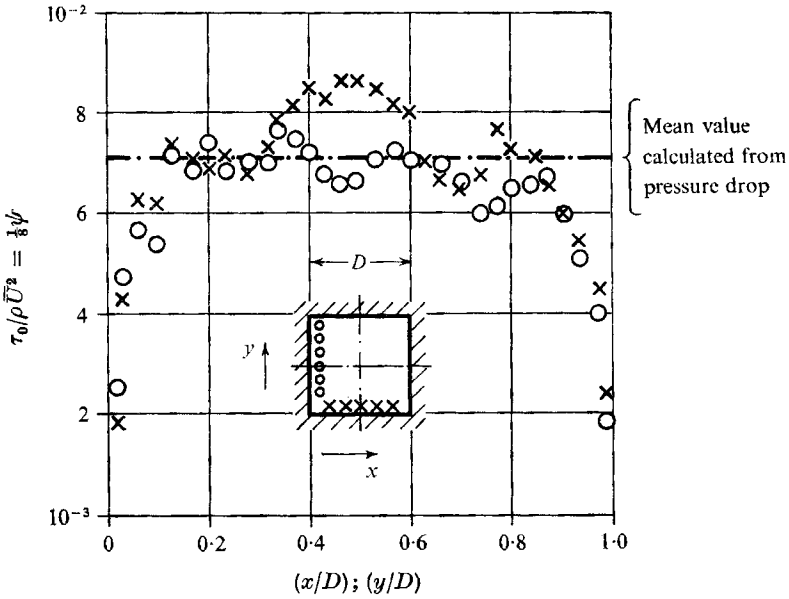

FIGURE 3. Local skin friction at the circumference of a square duct.
$Re = 6 \times 10^5$; $k_s/D = 450 \times 10^{-5}$.

4. Results

4.1. *Preliminary tests*

In this section results are given, which are to be considered in connexion with the calibrating method. Figure 3 shows the distribution of local skin-friction coefficient $(\tau_0/\rho\bar{U}^2) \equiv \frac{1}{8}\psi$ along the circumference of the cross-section (x/D), respectively (y/D) of the square duct. The curves refer to two neighbouring walls, perpendicularly situated to one another. Because of the secondary flow in the duct the profile is not uniform. Verifying the calibration of the surface edge, the real local values, measured with the calibrated Preston tube, are used. Figure 4 represents an example of the calibration curve obtained in the described way. The cross symbols refer to turbulent boundary layer and calibration by means of channel flow. The results signifying the laminar flow are calculated from the pressure distribution around the rough cylinder for the laminar part of the boundary layer. Both parts of the curve have been applied alternatively to the evaluation of the cross-flow around the cylinder depending on the character of the flow. In the lower region the laminar and turbulent curve

coincide. With increasing Reynolds number the values of the turbulent rough-channel flow are approaching a constant value; that means that the pressure difference felt at the edge is proportional to the local wall shear stresses.

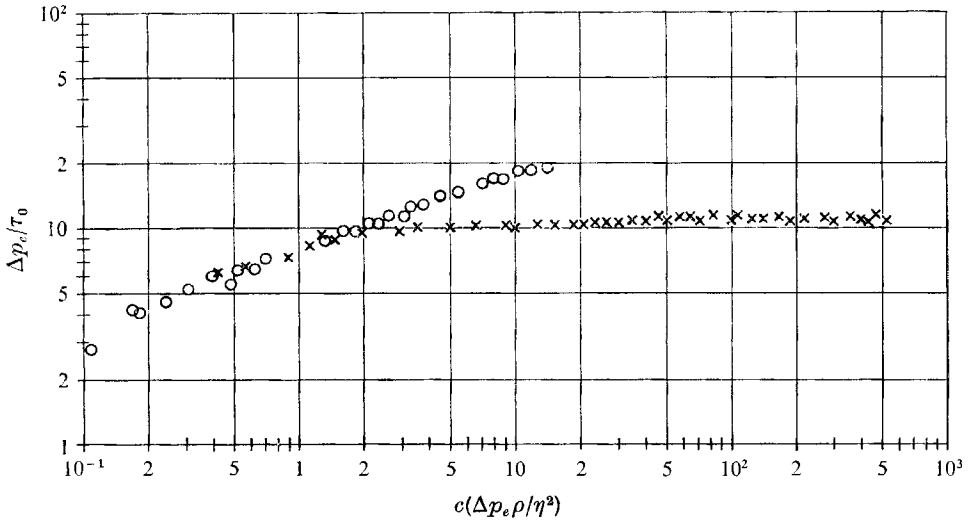

FIGURE 4. Calibration curve of the skin friction probe at $k_s/D = 450 \times 10^{-5}$. ×, turbulent; ○, laminar.

Figure 5 represents Nikuradse's (1933) famous diagram concerning the pressure loss of the flow through rough circular pipes. As mentioned above, this diagram was used to classify the roughness of our emery papers into the system of the equivalent sand-grain roughness. For this purpose the results of the rough square ducts are plotted into figure 5. On account of the constant friction factor at high Reynolds numbers the classification could easily be made by means of the auxiliary diagram (figure 6) derived from figure 5. The high Reynolds numbers ($Re > 6 \times 10^5$) were achieved by carrying out the experiments in the high-pressure wind tunnel.

4.2. *Drag coefficient*

In the range of Reynolds numbers $10^5 < Re < 3 \times 10^6$ local values of static pressure and skin friction have been measured as a function of the angle of circumference Φ. For Reynolds numbers $Re < 10^5$ the signal obtained from the skin friction probe was too small, so only the static pressure has been determined. The integration of the local stresses leads to the total drag coefficient c_d, which is shown in figure 7 depending on Reynolds number. The parameter is the roughness coefficient k_s/D. The results for the smooth cylinder which had a maximum total roughness height of 2 μm measured in axial direction are taken from earlier investigations (Achenbach 1968).

The curve representing the drag coefficient as a function of Reynolds number can be divided into four parts, as shown in figure 8. Each of these ranges is characterized by a special boundary-layer behaviour, which is discussed in the next

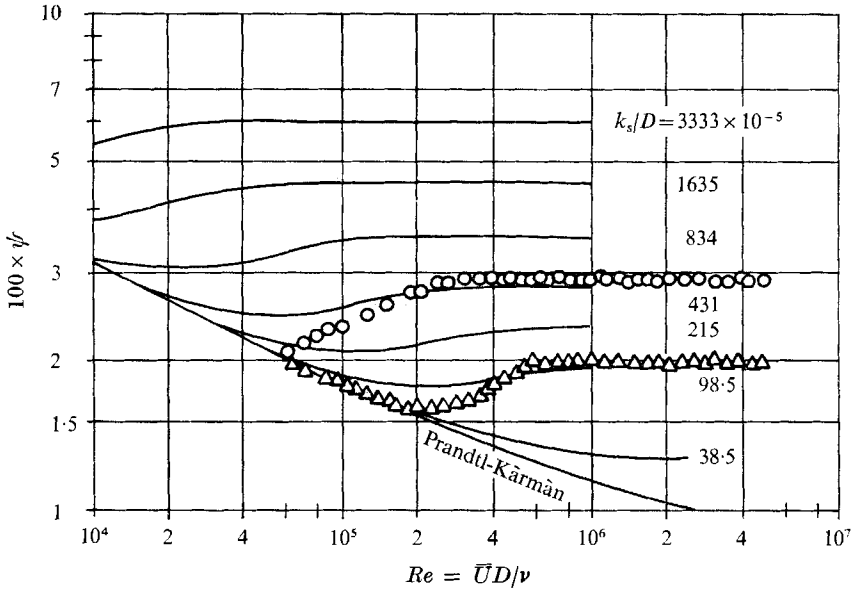

FIGURE 5. Pressure drop coefficient ψ of rough circular tubes (after Nikuradse 1933) and square ducts as function of Reynolds number.

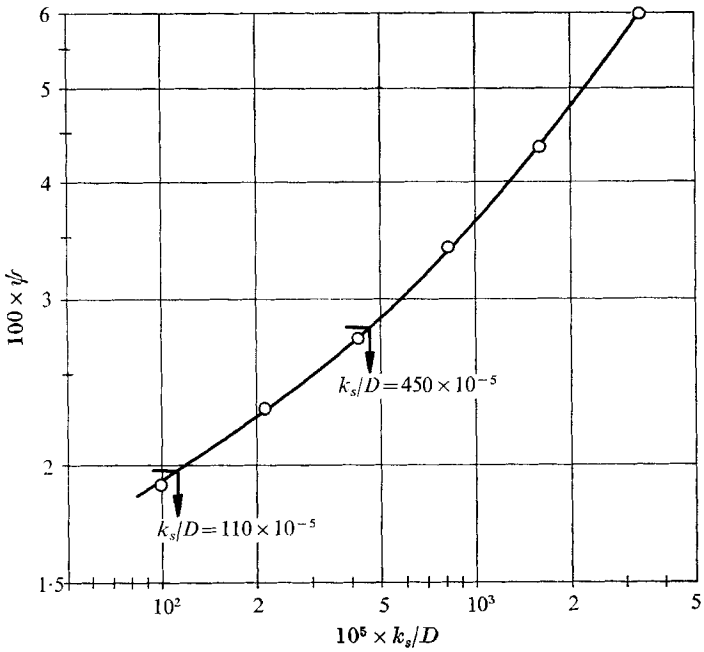

FIGURE 6. Pressure-drop coefficient of completely rough flow through circular pipes *versus* roughness parameter k_s/D (from Nikuradse).

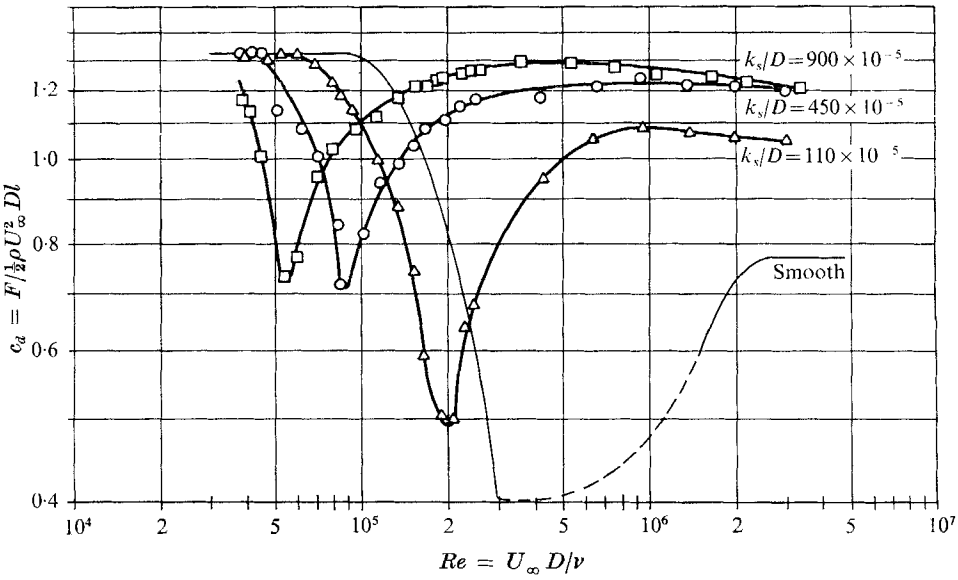

FIGURE 7. Drag coefficient of rough circular cylinders in cross-flow *versus* Reynolds number, uncorrected for blockage effects.

paragraph. The subcritical flow régime is not yet influenced by the surface roughness. In a large range of Reynolds number the drag coefficient is nearly constant. Increasing the Reynolds number the drag coefficient suddenly drops. This range, the lower limit of which is dependent upon the roughness conditions, is denoted the critical flow régime. Exceeding the Reynolds number of c_d minimum the drag coefficient grows up again (supercritical range) and reaches a nearly constant value in the transcritical range. This 'transcritical drag

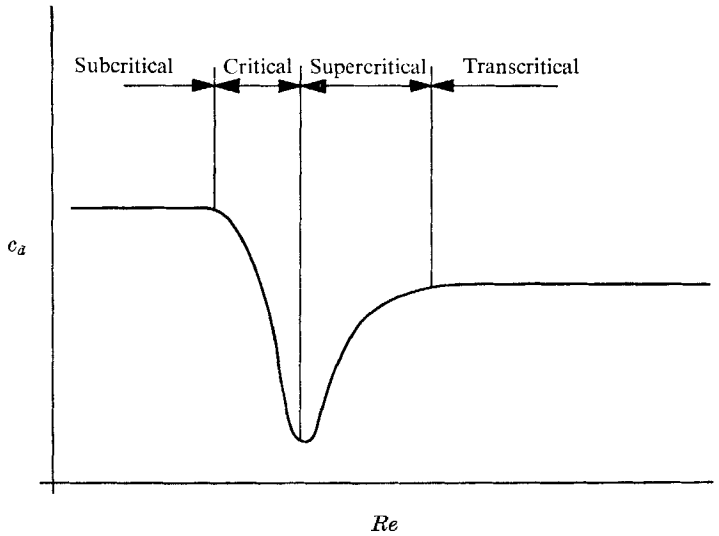

FIGURE 8. On the definition of the four flow ranges at the flow past circular cylinders.

coefficient' increases with rising roughness parameter. As no absolute values of wall shear stresses were available for the case of spherical roughness to calculate the drag coefficient, the percentage of friction forces was estimated to be 1 % in the subcritical flow régime and 3 % in the critical, supercritical and transcritical flow ranges.

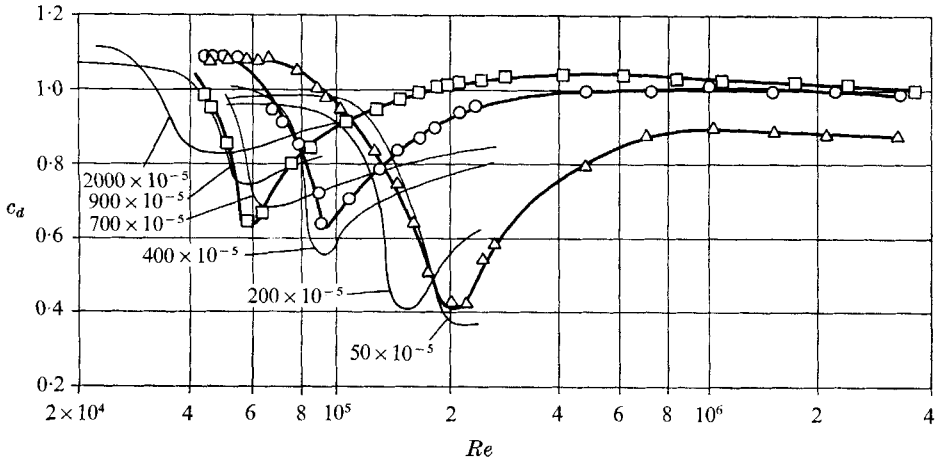

FIGURE 9. Corrected drag coefficient of rough circular cylinders in cross-flow. Comparison with results of Fage & Warsap (1930). △, $k_s/D = 110 \times 10^{-5}$; ○, $k_s/D = 450 \times 10^{-5}$; □, $k_s/D = 900 \times 10^{-5}$; ——, Fage & Warsap (1930).

The investigations have been made at a blockage ratio $D:B = 1:6$, where B is the width of the test section. Figure 9 shows the drag coefficient corrected according to the formula of Allen & Vincenti (1944). The correction was performed even in the region of strongly changing drag coefficient, though the application is rather doubtful here, as mentioned also by Roshko (1961). As to be seen from the example of the subcritical flow, where $c_d = 1{\cdot}2$ is expected, an over-correction occurs for our case of blockage ratio. Nevertheless, these values were compared with the likewise corrected results of Fage & Warsap (1930). It is remarkable that Fage & Warsap did not find any dependency of drag coefficient on blockage. Their uncorrected values measured for the blockage ratios $D:B = 1:6$, $D:B = 1:20$ coincide in the subcritical flow range. That means that the corrected curves split in this comparable region.

In their original paper Fage & Warsap (1930) gave no details concerning the relative roughness parameter k/D. Later on their results were cited by Schlichting (1964, p. 614), who added information about the surface conditions. Comparing those revised results with the present data the agreement is rather satisfying with regard to the investigations on emery paper. Applying the results of Fage & Warsap to our spherical roughness, the parameter would have the value $k_s/D \approx 900$ (figure 9). On the other hand the diameter of the glued spheres is $d = 2{\cdot}5$ mm. That leads to $k/D = 1650$, assuming that $k = d$. From this it can be concluded that for the case of circular cylinders the equivalent sand-grain roughness is not $1d$ but only $0{\cdot}55d$. In this connexion the investigations on the

flow through a rough square duct made by Schlichting (1936) should be mentioned. He found in his experiments carried out for the case of the most compact but regular arrangement of spheres at the surface of the square duct that the equivalent sand-grain roughness had a value of $k_s = 0{\cdot}627\,d$.

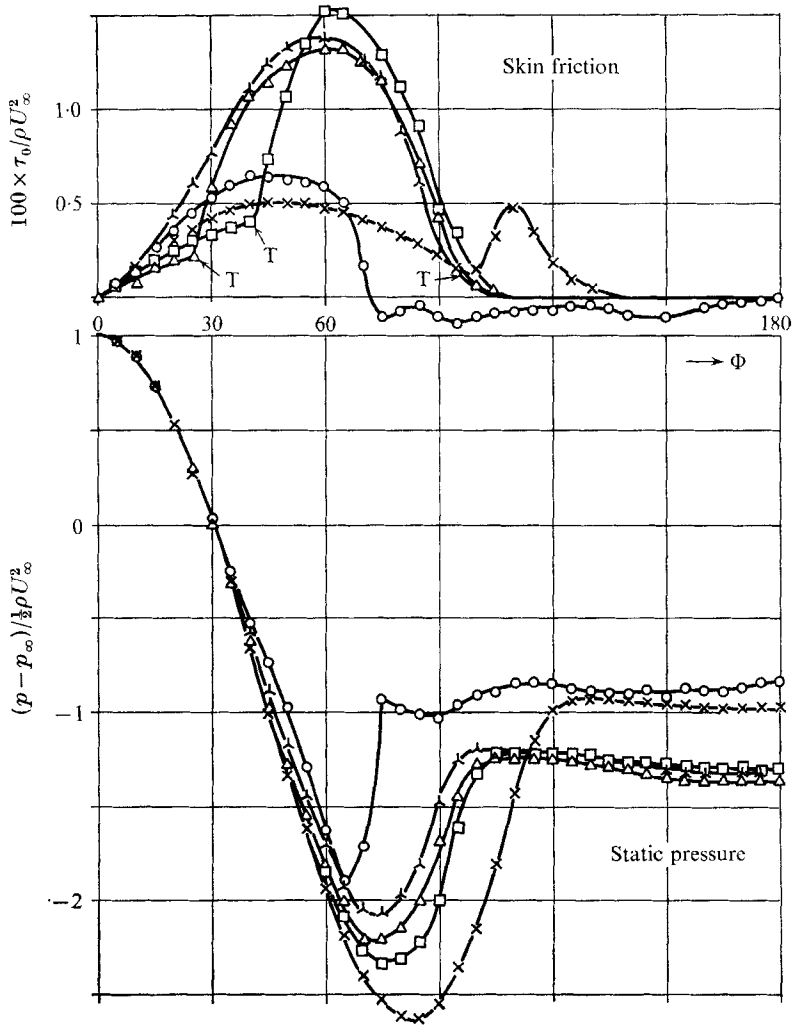

FIGURE 10. Local pressure and skin friction distribution of the rough circular cylinder in cross-flow ($k_s/D = 110 \times 10^{-5}$). Values uncorrected for tunnel blockage. 'T' means boundary-layer transition. *Re*: ○, $1{\cdot}3 \times 10^5$; ×, $2{\cdot}4 \times 10^5$; □, $4{\cdot}3 \times 10^5$; △, $6{\cdot}5 \times 10^5$; —⅄—, $3{\cdot}0 \times 10^6$.

4.3. *Local pressure and skin friction distribution*

Figures 10 and 11 show several characteristic distributions of local static pressure ($p - p_\infty$) and skin friction τ_0, valid for the two roughness grades investigated. The static pressure was made non-dimensional by the dynamic pressure ($\frac{1}{2}\rho U_\infty^2$), where U_∞ is the velocity of the undisturbed flow. In a similar way the local shear stresses were presented in a dimensionless form by using double the

dynamic pressure as reference pressure. The latter presentation results in this form from the momentum equation of the boundary layer. In that régime, where the flow is influenced by the roughness of the surface, the diameter of the cylinder is no longer the characteristic length. Therefore the normalizing factor

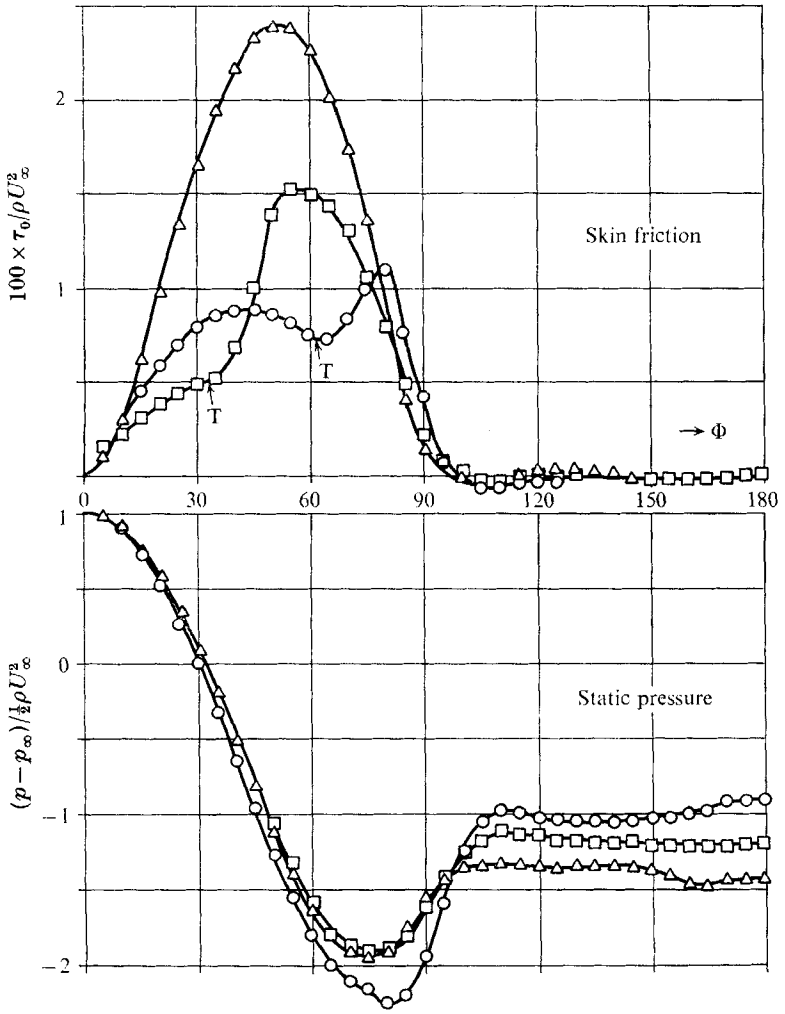

FIGURE 11. Local pressure and skin friction distribution of the rough circular cylinder in cross-flow ($k_s/D = 450 \times 10^{-5}$). Values uncorrected for tunnel blockage. 'T' means boundary-layer transition. *Re*: ○, $1{\cdot}0 \times 10^5$; □, $1{\cdot}7 \times 10^5$; △, $3{\cdot}0 \times 10^6$.

$[U_\infty . D/\nu]^{\frac{1}{2}}$, which is known from the laminar flow, does not appear as part of the friction coefficient. Of course, this presentation is not relevant for the subcritical flow along the rough surface, but it was applied to facilitate the comparison at various Reynolds numbers.

From the local pressure and skin friction distribution the behaviour of the boundary layer can be observed. The position of zero skin friction indicates the separation of the boundary layer. The transition from laminar to turbulent flow

is accompanied by a sudden rise of wall shear stresses. For angles of circumference greater than $\phi' = 25°$ the transition point can be determined with an uncertainty of only some degrees, assuming that the transition occurs at that position where the measured curve deviates from the suggested laminar trace. In figures 10 and 11 these points are denoted with 'T'. For angles smaller than $\phi = 25°$ the experimental determination of the transition point is of moderate accuracy, because the local gradient $(d\tau_0/d\phi)$ is too steep near the stagnation point.

The experiments show that in the subcritical flow régime the boundary layer separates laminarly in the front portion of the cylinder as a consequence of the friction forces. With increasing Reynolds number the ratio of inertial forces to friction forces grows up. Besides, the disturbances produced by the rough surface support the boundary layer with energy from outside. Thus these two effects cause the boundary layer to be adjacent to the wall over a larger distance. The shifting of the separation point to the back of the cylinder leads to a recovery of the base pressure and therefore to a reduction of the drag coefficient. However, the separation is still laminar. This critical flow range indicated by the sudden decrease of c_d is rather unstable and sensitive. Thus accidental disturbances cause an incalculable change of the flow. Probably this is the reason for the odd pressure distribution at $Re = 1{\cdot}3 \times 10^5$ in figure 10.

At the Reynolds number where c_d is minimum, laminar separation and turbulent reattachment occurs. This phenomenon of the so-called separation bubbles could be observed for the case of smooth surfaces in a large range of Reynolds numbers $(3 \times 10^5 < Re < 1{\cdot}5 \times 10^6)$. However, it is restricted to a narrow flow range if the surface of the cylinder is rough.

In the supercritical flow régime, where c_d is increasing again, an immediate transition from laminar to turbulent flow is to be observed. With increasing Reynolds number the transition point shifts from behind the main cross-section to the neighbourhood of the stagnation point. Finally the drag coefficient has reached a new plateau. The transcritical flow range is developed, where the entire boundary layer is turbulent except a small region near the stagnation point.

In figure 12 the shifting of the transition point as a function of Reynolds number is presented for the three roughnesses tested. Large roughness heights cause strong disturbances and therefore lead to premature transition.

Figure 13 gives information on boundary-layer separation. Corresponding to the magnitude of the drag coefficient the separation point moves between the front portion and the back side of the cylinder. Low drag coefficients mean large values of separation angles and vice versa.

4.4. *Friction forces*

Concerning the percentage of friction forces on the total drag, similar observations can be made both for the rough- and for the smooth-surfaced cylinder: in the range investigated friction forces contribute only a few per cent to the flow resistance. This result, which is illustrated in figure 14, can be obtained by the integration of the local pressure and skin friction forces. Whereas the percentage of friction diminishes for the case of the smooth cylinder in the

transcritical range with increasing Reynolds number, it remains at a nearly constant level for the rough cylinder. As the total drag coefficient has a constant value, this result is in good agreement with the suggestion that in the transcritical flow range the magnitude of wall shear stresses is independent of the Reynolds number $Re = U_\infty D/\nu$, but only a function of the roughness parameter k_s/D.

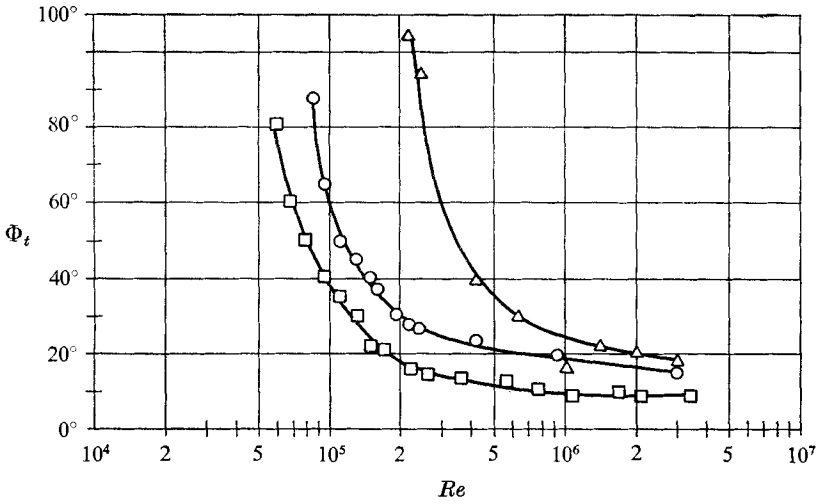

FIGURE 12. Circular cylinder in cross-flow. Angular position of transition laminar–turbulent at various roughness parameters. △, $k_s/D = 110 \times 10^{-5}$; ○, $k_s/D = 450 \times 10^{-5}$; □, $k_s/D = 900 \times 10^{-5}$.

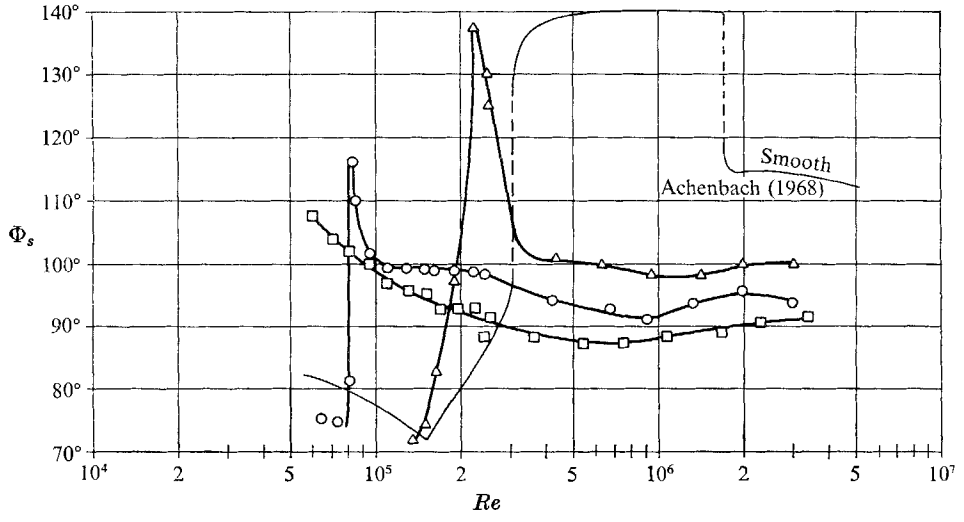

FIGURE 13. Circular cylinder in cross-flow. Angular position of boundary-layer separation at various roughness parameters. Symbols as in figure 12.

5. Concluding remarks

The actual results allow one to describe the phenomena, which occur at the cross-flow past rough cylinders. As known from earlier investigations, increasing roughness parameters cause decreasing critical Reynolds numbers. In the trans-critical flow régime higher drag coefficients correspond to higher roughness.

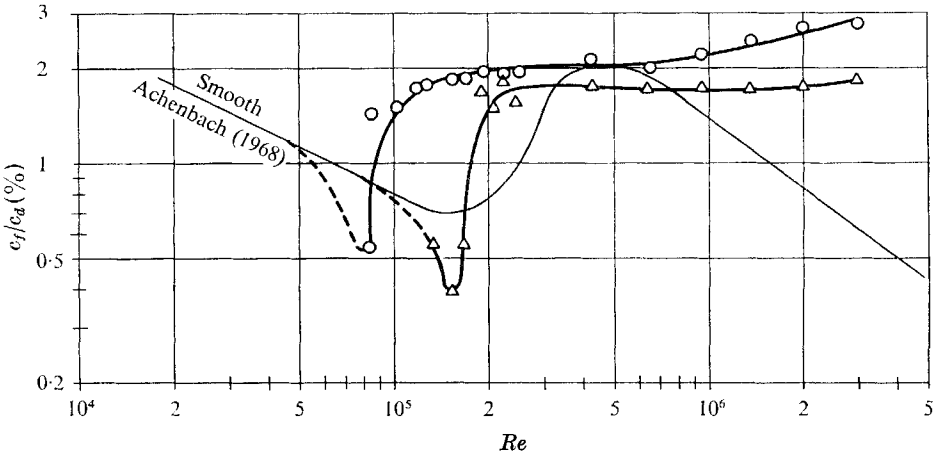

FIGURE 14. Circular cylinder in cross-flow. Percentage of friction forces with respect to the total drag. Symbols as in figure 12.

The roughness parameter k_s/D chosen in our presentation is of less physical meaning than of practical profit. From the physical point of view the boundary-layer thickness δ must be introduced as the reference length, so the roughness parameter might have the form k_s/δ. For the case of flow through pipes this definition leads to the expression $k_s/\delta = 2(k_s/D)$, where k_s/D then is a parameter physically relevant as well as practical. However, the boundary layer of the cylinder in cross-flow varies with angular position and Reynolds number. Therefore one prefers to introduce the diameter D as auxiliary characteristic length. Remembering this fact one understands that there is no direct physical relationship between the roughness parameter k_s/D valid either for the pipe or for the cylinder. On the other hand it must be expected that, on account of the thin boundary layers, still small roughness heights have an important effect on the flow.

The calibration of the skin-friction probe is considered to be a severe problem. The method used seemed to be the only practicable facility to get knowledge of the local wall shear stresses. Whereas the imponderables of the rough surface are included in the calibration curve by the transplantation method, the effect of variable pressure gradient could not be taken into account. However, the probes are of a similar small size as used for the measurements at the smooth cylinder. For that case the comparison with the theory showed a good reliability of the skin friction probe. This was the reason that we dared to apply the probe to the rough-surfaced cylinder, though being calibrated in a flow with small pressure gradient.

Besides the many difficulties which result from the statement of a uniform transplantable surface-roughness, there is at least one advantage: the problem of premature separation of the boundary layer effected by the probes is no longer essential, because the probes immerse into the roughnesses of the surface.

Considering figure 5 it is noticeable that in the region of transition from hydraulically smooth to completely rough channel flow, the friction coefficients show a behaviour different from Nikuradse's results. This effect is probably caused by the different characters of roughnesses investigated. An analogous influence can be observed comparing the drag coefficients of the cylinders roughened either by gluing spheres or emery paper.

The investigations have been carried out in the high-pressure wind tunnel of the Institut für Reaktorbauelemente der Kernforschungsanlage Jülich, Bundesrepublik Deutschland. The author wishes to thank all co-workers, who made a contribution to a successful performance of the experiments. Especially he wants to express his gratitude to H. Gillessen, F. Hoffmanns, H. Reger, W. Schmidt and G. Türk, who undertook responsibility for the preparation and conduction of the investigations.

REEERENCES

ACHENBACH, E. 1968 Distribution of local pressure and skin friction around a circular cylinder in cross-flow up to $Re = 5 \times 10^6$. *J. Fluid Mech.* **34**, 625–639.

ALLEN, H. J. & VINCENTI, W. G. 1944 Wall interference in a two-dimensional-flow wind tunnel, with consideration of the effect of compressibility. *Nat. Adv. Comm. Aero. Wash., Rep.* 782.

FAGE, A. & WARSAP, J. H. 1930 The effect of turbulence and surface roughness on the drag of a circular cylinder. *Aero. Res. Com. London, R. & M.* no. 1283.

NIKURADSE, J. 1933 Strömungsgesetze in rauhen Rohren. *Forsch. Arb. Ing.-Wes. Heft* 361.

ROSHKO, A. 1961 Experiments on the flow past a circular cylinder at very high Reynolds number. *J. Fluid Mech.* **10**, 345–356.

SCHLICHTING, H. 1936 Experimentelle Untersuchungen zum Rauhigkeitsproblem. *Ing.-Arch.* 1–34. Translation: *Proc. Soc. Mech. Eng. USA* (1936).

SCHLICHTING, H. 1964 *Grenzschicht-Theorie.* G. Braun.